Journal of Hazardous Materials 167 (2009) 879–884

Contents lists available at ScienceDirect

Journal of Hazardous Materials

journal homepage: www.elsevier.com/locate/jhazmat

Conductive carbon–clay nanocomposites from petroleum oily sludge

Patricia Fernanda Andrade[a], Thiago Figueiredo Azevedo[b], Iara F. Gimenez[a,b], Antonio Gomes Souza Filho[c], Ledjane Silva Barreto[a,b,*]

[a] Núcleo de Pós-graduação em Química, Universidade Federal de Sergipe- UFS, Av. Marechal Rondon s/n, São Cristóvão 49100-000, SE, Brazil
[b] Núcleo de Ciência e Engenharia de Materiais, Universidade Federal de Sergipe- UFS, Av. Marechal Rondon s/n, São Cristóvão 49100-000, SE, Brazil
[c] Departamento de Física, Universidade Federal do Ceará, Caixa Postal 6030, Fortaleza, Ceará, CEP 60450-900, Brazil

ARTICLE INFO

Article history:
Received 11 August 2008
Received in revised form 16 January 2009
Accepted 20 January 2009
Available online 3 March 2009

Keywords:
Solid waste
Carbon
Clay
Composite
Impedance

ABSTRACT

Oily sludge samples formed in water–oil separation tanks from a petroleum industry were collected, characterized and heat-treated at different temperatures, in order to yield carbon–clay composites. EDX microanalysis, XRD and FTIR data revealed that before carbonization the oily sludge was formed mainly by a mixture of quartz, montmorillonite, calcite, barite and oil residues. After carbonization, mineral phases present were mainly quartz, anorthite and gehlenite, in addition to graphitic and disordered carbon domains, according to XRD, Raman and TEM measurements. A preliminary evaluation of the electrical conductivity performed by Impedance Spectroscopy revealed that the composites formed are conductive, exhibiting conductivity values typical of semiconductors, in contrast to the precursor material.

1. Introduction

The petroleum industry generates large amounts of solid and semisolid wastes known as oily sludges, which are formed by oil residues coalesced on fine solids [1]. Those sludges can be generated in several steps of the petroleum production and refining, such as in oil/water separation steps and in the bottom of tanks. Since oily sludges are considered hazardous wastes that can affect groundwater and soil resources, their management must follow restrictive specifications from regulatory agencies. However, as options for oily sludge disposal are limited and the volumes of generated wastes are very high, the situation gives rise to a heavy burden for the petrochemical industries [1]. Disposal in landfills is not successful since an oil content of <1% is required and incineration may cause air pollution with no energy advantage. Thus stabilization and recycling are considered suitable environmental alternatives for the management of those solid wastes.

In this context Voudrias and co-workers reported the cement-based solidification/stabilization of oily sludges and studied leaching behavior of hydrocarbons, concluding that cement addition caused destabilization of the oily sludge in terms of durability [2]. Al Hamdi and co-workers studied the recycling of oily sludge in asphalt paving mixtures with positive results for samples containing up to 22% oily sludge in terms of the desired stability and flow properties [3]. An alternative that is promising for reusing a wide variety of wastes, ranging from agricultural ones [4,5] to sewage and petrochemical residues is the production of carbon materials and composites. Several wastes from the petrochemical industry have been tested for this purpose, such as biosolids and biosludges formed in biological wastewater treatment plants used as raw materials for the fabrication of mesoporous activated carbons with $ZnCl_2$ as activating agent [6]. In a subsequent work the activated carbons obtained were tested for adsorption of benzene, with the possibility of desorption and reuse [7]. The use of petroleum coke produced as waste in a Mexican petroleum refinery as raw material for activated carbon was reported for application in treatment of heavy metal-containing wastewater [8]. Bottom of barrel wastes from a Mexican plant were also used for production of activated carbons viability in desulphuration adsorption of fuel gas [9].

The preparation of activated carbons and composites for applications other than adsorption is also an area of great opportunities. It has been reported that carbon–clay composites may exhibit an electrical conductivity dependent on the thermal treatment temperature and that the layered structure of the clay determines the conductivity [10]. These materials can be applied in capacitors, electrocatalysts and sensors [11] as well as supports for composite preparation owing to the controllable carbon porosity [12].

In this work we characterized an oily sludge formed in water/oil separators from a local petroleum industry and heated this residue

* Corresponding author at: Núcleo de Ciência e Engenharia de Materiais, Universidade Federal de Sergipe- UFS, Av. Marechal Rondon s/n, São Cristóvão 49100-000, SE, Brazil. Fax: +55 79 21056845.
E-mail address: ledjane@ufs.br (L.S. Barreto).

0304-3894/$ – see front matter © 2009 Elsevier B.V. All rights reserved.
doi:10.1016/j.jhazmat.2009.01.070

under different conditions for carbonization, aiming to obtain conductive carbon–clay nanocomposites. The chemical composition, crystalline phases, and microstructure of the samples were characterized before and after thermal treatment and the electrical conductivity of pyrolyzed samples were evaluated by impedance spectroscopy.

2. Experimental

2.1. Materials

Oily sludge samples used in this work were collected in the wastewater treatment plant from a local industry at the state of Sergipe/Brazil.

2.2. Sample treatment

The as-received samples were centrifuged at 25,000 rpm for 15 min at room temperature for removal of oil excess. Solid sludge collected after centrifugation was dried at 110 °C for 24 h and sieved with 65 mesh sieve (this sample was labelled: "dry sludge"). Then the solids were heated at a 10 °C/min rate up to 800 °C under N_2 and pyrolyzed at this condition for 2 h (sample: "carbonized sludge"). In order to study structure evolution upon heating, samples were heated under N_2 at the following temperatures: 400 °C, 500 °C, 600 °C, 700 °C and 900 °C.

2.3. Characterization

Dry and carbonized sludge samples were characterized by scanning electron microscopy (SEM) in a JEOL-JSM-6360LV microscope coupled to an EDX analytical microprobe and by scanning transmission electron microscopy (STEM) LEO-910 microscope, operating at an accelerating voltage of 80 kV. Samples heated at 400 °C, 500 °C, 600 °C, 700 °C, 800 °C, and 900 °C were characterized by powder X-ray diffractometry using a RIGAKU diffractometer with a Cu Kα (λ = 1542 Å) source. Samples heated at different temperatures were also characterized by Fourier transform infrared (FTIR) spectra of KBr discs, recorded in a PerkinElmer Spectrum BX spectrophotometer in the range between 400 and 4000 cm^{-1} with 4 cm^{-1} resolution. Surface area and porosity measurements for dry and carbonized sludge were carried out by N_2 adsorption at 77 K using a Quantachrome Instruments, Autosorb-1C. Thermogravimetric analysis measurements (TG) were performed using a TA SDT 2960 instrument with 10 °C/min heating rate up to 1200 °C under N_2 flow (100 mL/min) in platinum pans. Raman spectra for the carbonized sludge were recorded with Jobin Yvon T64000 instrument coupled to a CCD detector and using an argon laser (λ = 514.5 nm) with a power of 1 mW. For impedance measurements pellet samples of 6 mm diameter and 1 mm thickness were placed in a Solartron 1260 impedancimeter in the 1 Hz to 13 MHz frequency range at room temperature. Data were treated with Zview software.

3. Results and discussion

A semi quantitative chemical analysis of dry and carbonized sludges, Table 1, was obtained from the EDX analyzer coupled to SEM measurements. It is worth to mention that elements such as Fe/F and Ti/Ba are indistinguishable in the 1–10 keV range, so the values assigned in the table as F and Ti are probably related to Fe and Ba, respectively. The results indicate that both samples present relatively high carbon content in addition to mineral components, which were properly identified by XRD measurements. The relative amount of carbon decreases after carbonization, as expected considering the decomposition of the organic components. It is worth to note that the amount of toxic species such as barium did not vary upon carbonization, suggesting its stabilization in the carbonized sludge. Oscillation in the percent amounts of the elements may arise from the multiphase character of the samples. As will be seen in the XRD discussion, all elements found can be well distributed among the crystalline phases. Before carbonization: barite ($BaSO_4$), calcite ($CaCO_3$), montmorillonite ($(Na,Ca)1/3(Al,Fe)Mg_2(Si_4O_{10})(OH)_2{\cdot}nH_2O$), quartz ($SiO_2$). After carbonization: quartz and cristobalite (SiO_2), wollastonite

Table 1
Chemical analysis data from EDX measurements for dry and carbonized sludge.

Element	Dry sludge		Carbonized sludge	
	Mass (%)	Atom (%)	Mass (%)	Atom (%)
C	46	61	23	37
O	27	28	32	39
F	Trace	Trace	1	1
Na	1	1	1	1
Mg	1	1	2	2
Al	2	1	4	3
Si	5	3	9	6
S	2	1	2	1
Cl	1	1	3	2
K	1	0	1	1
Ca	2	1	9	4
Ti	Trace	Trace	1	0
Fe	4	1	4	2
Cu	1	0	1	0
Ba	6	1	6	1
Total	100	100	100	100

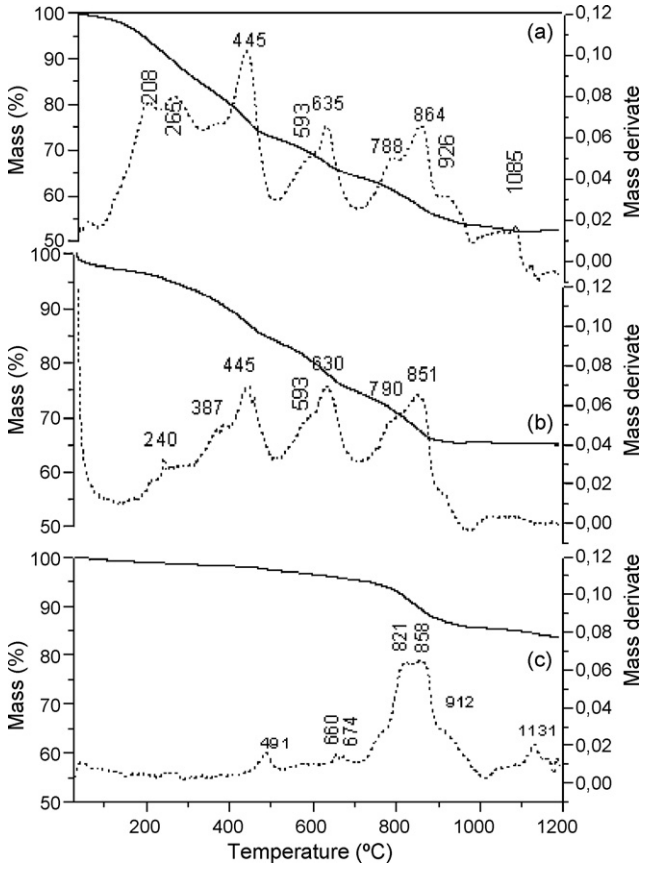

Fig. 1. TG (solid lines) and DTG (dotted lines) curves for: (a) dry oily sludge, (b) oily sludge washed with hexane, (c) carbonized sludge.

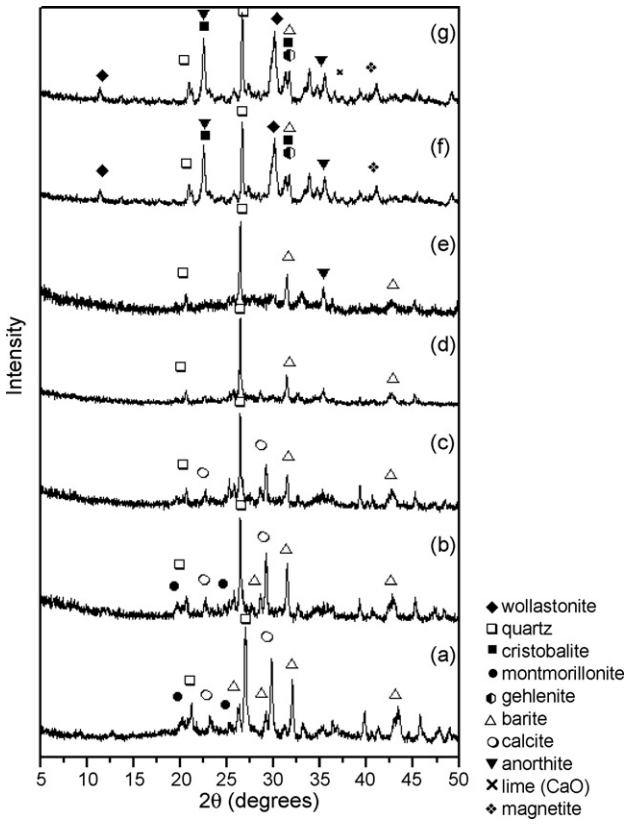

Fig. 2. Powder XRD pattern for: dry oily sludge (a) and oily sludge carbonized at different temperatures: 400 °C (b), 500 °C (c), 600 °C (d), 700 °C (e), 800 °C (f), and 900 °C (g). Q = quartz, M = montmorillonite, C = calcite, B = barite, A = anorthite, G = gehlenite. JCPDS cards: Anorthite (41-1486); cristobalite (11-695; gehlenite $Ca_2Al_2SiO_7$ (35-755), calcium oxide (28-0775), wollastonite (76-0186), Quartz (46-1045), calcite (5-586), barite (24-1035), Montmorillonite (12-219), magnetite (19-0629).

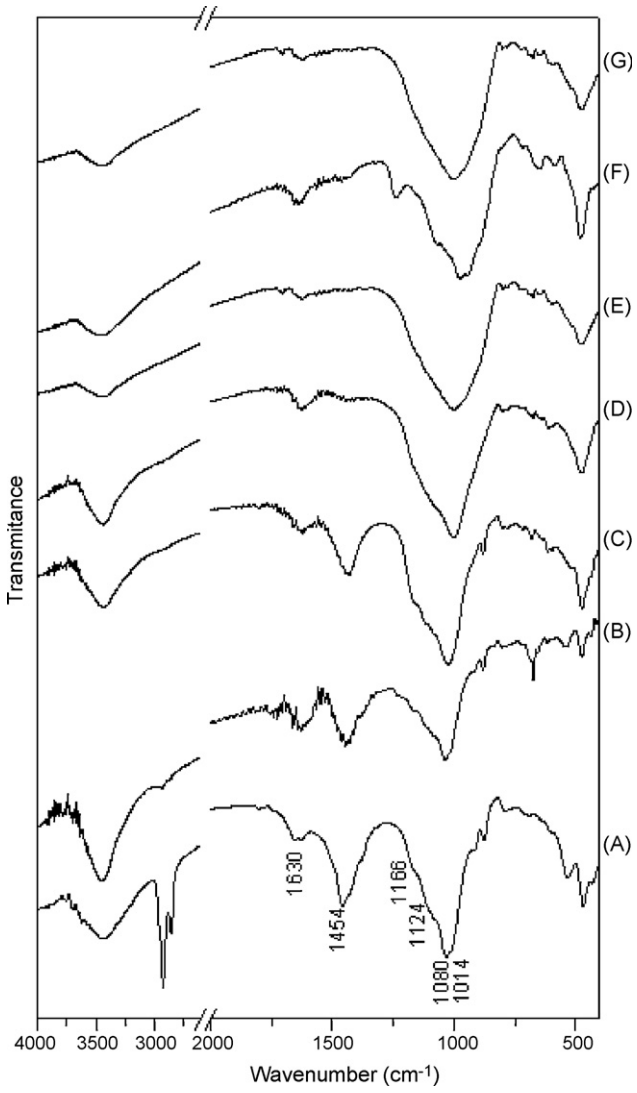

Fig. 3. FTIR spectra for: dry oily sludge (a) and oily sludge carbonized at different temperatures: 400 °C (b), 500 °C (c), 600 °C (d), 700 °C (e), 800 °C (f), and 900 °C (g).

($CaSiO_3$), anorthite ($CaAl_2Si_2O_8$), gehlenite ($Ca_2Al_2SiO_7$), magnetite (Fe_3O_4) and lime (CaO).

The thermal behavior of the dry and carbonized sludge was studied by TG analysis, Fig. 1. The TG curve of the dry oily sludge exhibits a gradual mass loss with several steps, according to the DTG curve. These steps include decomposition of the oil residue, at 208 and 265 °C and of different mineral phases present, at higher temperatures. In order to clarify the decomposition of the oily content, a sample of oily sludge was centrifuged and washed several consecutive times with hexane. Its TG curve is presented in Fig. 1b. The only significant difference relative to the dry sludge is the decrease of the oil decomposition peak in the DTG curve (around 240 °C). Concerning to the mineral content, samples contain a mixture of phases such as montmorillonite, calcite and barite, among other, as will be shown in the XRD discussion. The thermal decomposition of those phases is described in the literature: montmorillonite starts to decompose at approximately 360 °C to 560 °C; calcite and other carbonates decompose in the range from 550 °C to 980 °C [13] and sulfates like barite only above 950 °C to 1180 °C [14]. Decomposition steps can be observed in these ranges in DTG curves. In the TG curve of the carbonized sludge, the total mass loss is severely reduced and small mass loss around 400 °C can be related to dehydroxylation of residual clays minerals. Above 700 °C a mass loss analogous to that observed for the dry sludge is observed, which can be assigned to remaining of the mineral phases cited above.

As the decomposition of the oil residue can be observed in the TG curves, an estimation of the carbon amount in the samples could in principle be proposed from this result. However, two points should be considered. First, the carbon percent detected by EDX analysis is still relatively high in the carbonized samples, indicating that the decomposition of the organic part is only partial. Second, most of the oil fraction in the whole industrial waste was removed by centrifugation as a pre-treatment before carbonization. Thus the oil fraction depends mostly on the pre-treatment conditions and is only partially decomposed in the heat treatment.

The crystalline phases present in the dry sludge and in the samples heated at different temperatures under N_2 were identified by X-ray diffractometry, Fig. 2. The dry sludge presents mainly quartz (peaks at $2\theta = 21°$, 23.1° and 26.6°), montmorillonite (composition variable; general composition $Ca_{0.5}Al_2Si_4O_{10}(OH)_2{\cdot}H_2O$ peaks at $2\theta = 19.9°$ and 25.5°), barite $BaSO_4$ (peaks at $2\theta = 26.2°$, 29.1° and 31.9°) and calcite $CaCO_3$ (peaks at $2\theta = 29.8°$, 23.1° and 26.6°), among other small unidentified peaks. Upon heating, peaks of montmorillonite and calcite start to disappear from 500 °C and those of barite show a slight decrease up to 700 °C, concomitant to the arising of anorthite $CaAl_2SiO_7$ (peaks at $2\theta = 22.2°$, 30.1° and 35.5°) and gehlenite $Ca_2Al_2SiO_8$ (peak at $2\theta = 31.3°$) above 800 °C, both found in ceramic materials [15], and in addition to α-cristobalite (SiO_2), wollastonite $CaSiO_3$ and magnetite Fe_3O_4. Previous works [16,17] describe that clays minerals such as montmorillonite, kaolinite, illite and others react with

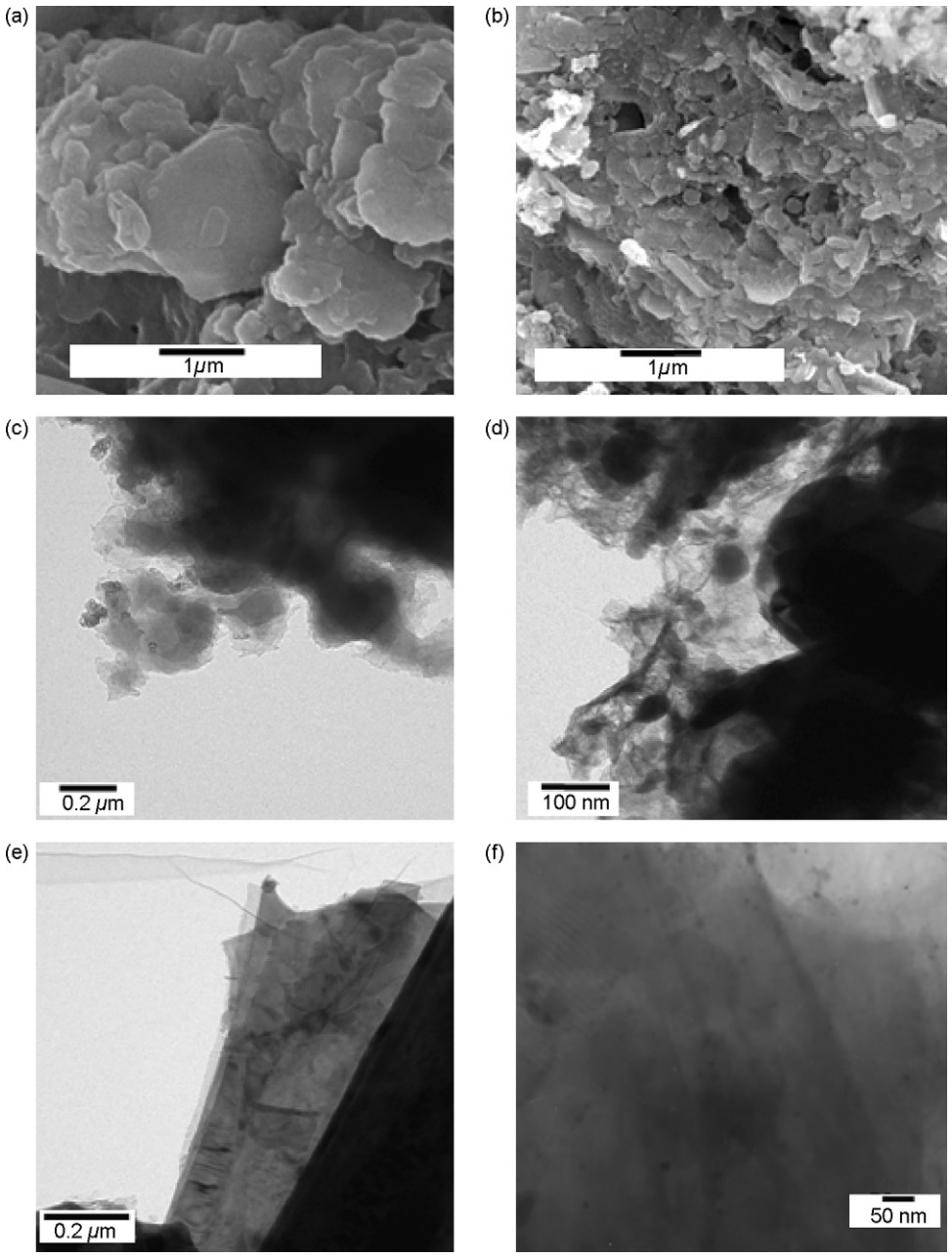

Fig. 4. SEM images for the dry (a) and carbonized sludge (b) and TEM images for the dry (c) and carbonized sludge (d–f).

calcium-containing minerals giving gehlenite, which can be further converted to anorthite. However, as the composition of clays minerals varies over a wide range, the exact reactions are not always proposed in the literature. We believe that in our case, the formation of gehlenite and anorthite both takes place with the reaction of montmorillonite and calcium-containing minerals such as calcite, leading to the formation initially of gehlenite (and probably cristobalite and CaO). Gehlenite can be afterwards converted to anorthite. In our samples, some XRD peaks can be assigned simultaneously to cristobalite and anorthite, thus the assignments are only tentative.

The main crystalline phases identified by X-ray diffractometry were confirmed by FTIR spectroscopy, Fig. 3. In the spectrum of dry sludge, the bands at 1166 cm^{-1} can be assigned to Si-O stretching from quartz. Bands at 1124 cm^{-1} and 1014 cm^{-1} can be assigned to Si-O stretching from montomorillonite, while the band at 1080 cm^{-1} is assigned to S–O bond stretching from barite ($BaSO_4$). In general, the band at 1630 cm^{-1} in spectra of clays minerals is assigned to the bending mode of adsorbed water molecules [13], but could be assigned also to C=C bonds from the organic residues. During thermal treatment structural transformations take place causing changes in the 900–1200 cm^{-1} spectral range, mainly as a consequence of the transformations of clays minerals identified by XRD as well as the organic matter decomposition.

The morphological changes of the dry and carbonized sludge were examined by scanning and transmission electron microscopies, Fig. 4. The SEM image of the dry sludge (Fig. 4a) is characterized by aggregates of flat plates with irregular boundaries and variable sizes. After carbonization at 800 °C the presence of thin particles of variable size can be observed in addition to relatively large blocks (Fig. 4b). TEM images reveal that before heating the dry sludge contains uniformly compact masses (Fig. 4c) and after carbonization the presence of dense particles dispersed along a less dense material (Fig. 4d), probably the carbonaceous phase.

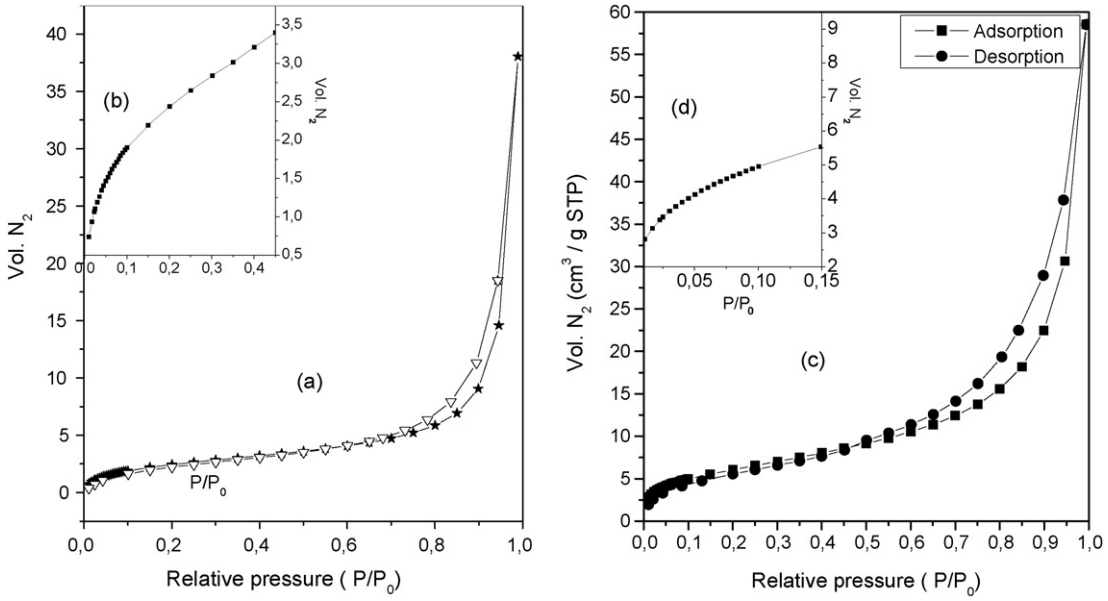

Fig. 5. Nitrogen adsorption isotherms for the dry sludge (a and b) and carbonized sludge (c and d).

A more detailed view of the TEM image of the carbonized sludge (Fig. 4e and 4f) evidence the presence of sheets (probably related to mineral structures) and particles with parallel planes, which can be assigned to graphitic crystallite domains.

Nitrogen adsorption measurements were carried out in order to address the evolution of the surface area and porosity with heating for the dry and carbonized sludge. For the dry sludge, Fig. 5a, gas adsorption is significant at relatively low pressures in the range 0 to 0.45, with a subsequent low inclination of the curve at intermediate pressures, indicating the predominance of micropores. For the carbonized sludge an increasing gas adsorption is observed at very low relative pressures, even lower than for the dry sludge. The curve profile has a slight inclination for intermediate relative pressures, but it is also indicative of a microporous material. For both samples the observation of a slight hysteresis (type H4) suggests the presence of sharp and slit shaped micropores. Surface area of dry sludge was 9.5 m^2/g, slightly increasing to 37 m^2/g after heating at 800 °C, probably as a result of pore formation upon decomposition of organic matter.

In order to get further insight into the structure of the carbon phase in the carbonized samples we measured space-resolved Raman spectra, which is a technique of great sensitivity to the structures of carbon and related materials. From this technique it is possible to evaluate the ordered and disordered carbon domains in the structure of a multiphase material, as well as to calculate the size of graphite crystallites with great accuracy [18]. Fig. 6 shows the Raman spectra of the carbonized sludge measured on two points of the sample, both showing two bands, as typical of disordered carbons with ordered crystallites. The band at 1597/1598 cm^{-1} is known as G band and is related to the presence of graphitic crystallites. The band at 1343/1344 cm^{-1} is labeled D band (disorder) and is related to disordered carbon structures. The intensity ratio of these two bands has been used to calculate the size of graphite crystallites in several papers. Cançado and co-workers proposed a general expression for the calculation of the size of graphite crystallites independently on the energy used in the excitation [19]. From this expression we estimated an average nanocrystal size of 12 nm and 9 nm for spectrum (a) and (b), respectively.

Finally a preliminary evaluation of the electrical properties of the carbonized sludge was carried out by complex impedance spectroscopy at room temperature, yielding the Nyquist plot shown

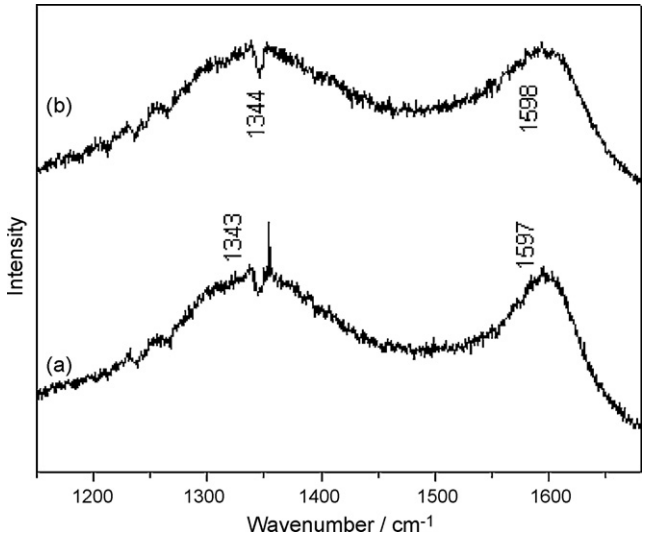

Fig. 6. Raman spectra obtained at different regions of the carbonized sludge's surface.

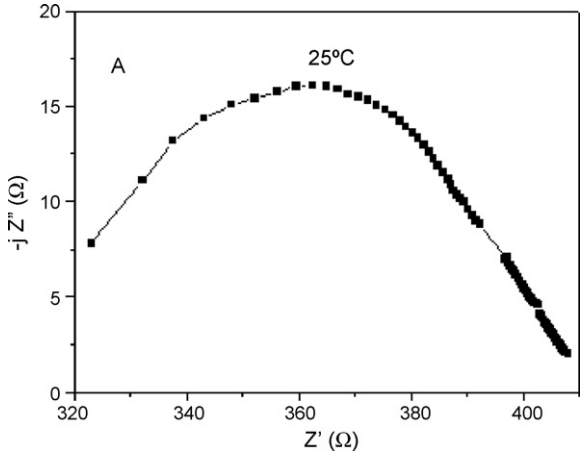

Fig. 7. Nyquist plot obtained from impedance spectroscopy measurements at room temperature for the carbonized sludge.

in Fig. 7. It is worth to mention that the dry sludge yielded no signal on this measurement, pointing out that the electrical conductivity is observed only after heating. An electrical conductivity of $8.65 \times 10^{-4}\ \Omega^{-1}\ cm^{-1}$, in the range of semiconductors, was calculated from the obtained impedance (408.7 Ω) by the expression:

$$C(\Omega^{-1}\ cm^{-1}) = \frac{d}{AZ}$$

where d = sample thickness (cm); A = area of the circular gold layer deposited on the sample surface (cm^2); Z = Impedance (Ω).

Further studies are in progress to evaluate the dependence of conductivity with temperature and with preparation conditions, in addition to applications in devices.

4. Conclusions

As the main conclusion of this work we emphasize that a material with interesting conductive properties can be prepared from a hazardous industrial waste. The results presented here provide an alternative to avoid the accumulation of solid wastes in landfills, in addition to potential applications of the material in sensors, catalysits and electronic devices.

Acknowledgements

Authors are grateful to Capes and Fapitec-SE for financial support and to Prof. G.D.A. Soares (PEMM-Coppe-UFRJ), to P. Aranda and E. Ruiz-Hitzky (ICMM-CSIC) for SEM and TEM measurements. A.G.S.F. acknowledges the support from Brazilian agency CNPq Grant No. 306335/2007-7.

References

[1] M. Elektorowicz, S. Habibi, Sustainable waste management: recovery of fuels from petroleum sludge, Can. J. Civ. Eng. 32 (2005) 164–169.
[2] A.K. Karamalidis, E.A. Voudrias, Cement-based stabilization/solidification of oil refinery sludge: leaching behavior of alkanes and PAHs, J. Hazard. Mater. 148 (2007) 122–135.
[3] R. Taha, M. Ba-Omar, A.E. Pillay, G. Roos, A. Al-Hamdi, Recycling of petroleum-contaminated sand, J. Environ. Monit. 3 (2001) 417–422.
[4] J.S. Macedo, N.B. Costa Junior, L.E. Almeida, E.F.S. Vieira, A.R. Cestari, I.F. Gimenez, N.L.V. Carreno, L.S. Barreto, Kinetic and calorimetric study of the adsorption of dyes on mesoporous activated carbon prepared from coconut coir dust, J. Colloid Interface Sci. 298 (2006) 515–522.
[5] J.S. Macedo, L. Otubo, O.P. Ferreira, I.F. Gimenez, I.O. Mazali, L.S. Barreto, Biomorphic activated porous carbons with complex microstructures from lignocellulosic residues, Microporous Mesoporous Mater. 107 (2008) 276–285.
[6] H.L. Chiang, C.G. Choa, S.Y. Chen, M.C. Tsai, The reuse of biosludge as an adsorbent from a petrochemical wastewater treatment plant, J. Air Waste Manag. Assoc. 53 (2003) 1042–1051.
[7] H.L. Chiang, K.H. Lin, C.Y. Chen, C.G. Choa, C.S. Hwu, N. Lai, Adsorption characteristics of benzene on biosolid adsorbent and commercial activated carbons, J. Air Waste Manag. Assoc. 56 (2006) 591–600.
[8] R.M.R. Zamora, R. Schouwenaars, A.D. Moreno, G. Buitron, Production of activated carbon from petroleum coke and its application in water treatment for the removal of metals and phenol, Water Sci. Technol. 42 (2000) 119–126.
[9] R. Pulido, G. Fernandez, Mexican bottom of barrel life cycle environmental proposal, Energy 32 (2007) 619–626.
[10] F. Montilla, E. Morallon, J.L. Vazquez, J. Alcañiz-Monge, D. Cazorla-Amorós, A. Linares-Solano, Carbon-ceramic composites from coal tar pitch and clays: application as electrocatalyst support, Carbon 40 (2002) 2193–2200.
[11] A. Abbaspour, A. Izadyar, Platinum electrode coated with a bentonite-carbon composite as an environmental detection sensor detector of lead, Anal. Bioanal. Chem. 386 (2006) 1559–1565.
[12] T.J. Bandosz, J. Jagiello, K. Putyera, J.A. Schwarz, Pore structure of carbon-mineral nanocomposites and derived carbons obtained by template mineralization, Chem. Mater. 8 (1996) 2023–2029.
[13] S. Mukherjee, S.K. Srivastava, Minerals transformations in northeastern region coals of India on heat treatment, Energy Fuels 20 (2006) 1089–1096.
[14] B.V. L'vov, V.L. Ugolkov, Kinetics of free-surface decomposition of magnesium and barium sulfates analyzed thermogravimetric ally by the third-law method, Thermochim. Acta 411 (2004) 73–79.
[15] A.C.S. Alcantara, M.S.S. Beltrao, H.A. Oliveira, I.F. Gimenez, L.S. Barreto, Characterization of ceramic tiles prepared from two clays from Sergipe - Brazil, Appl. Clay Sci. 39 (2008) 160–165.
[16] S. Iwamoto, T. Sudo, Chemical reactions among clay minerals, calcium carbonate, and ammonium chloride, Am. Mineral. 50 (1965) 883–899.
[17] A.P. Routsala, Solid state formation of anorthite from some clay mineral-calcium mineral mixtures, Am. Mineral. 48 (1963) 792–803.
[18] M.A. Pimenta, G. Dresselhaus, M.S. Dresselhaus, L.G. Cancado, A. Jorio, R. Saito, Studying disorder in graphite-based systems by Raman spectroscopy, Phys. Chem. Chem. Phys. 9 (2007) 1276–1291.
[19] L.G. Cançado, K. Takai, T. Enoki, M. Endo, Y.A. Kim, H. Mizusaki, A. Jorio, L.N. Coelho, R. Magalhaes-Paniago, M.A. Pimenta, General equation for the determination n of the crystallite size La of nanographite by Raman Spectroscopy, Appl. Phys. Lett. 88 (2006) 163106.